by assuming different magnitudes of this energy inherent in different substrate molecules can the substituent effects on the heat of reaction be reconciled properly.

Finally, some comments on the symmetry factor involved in the rate constants seem to be in order. In calculating the bimolecular rate constant k for reaction 3, we have used the symmetry numer $\sigma = 4$ for the isolated ethylene molecule. Because the transition state is planar symmetric (C_s), its symmetry number is $\sigma = 2$. Therefore, the rate constants calculated from the TST involve a substrate symmetry factor of $^4/_2 = 2$. This is tantamount to stating that the k values calculated are in reality the sum of those for the structurally equivalent two carbon atoms. In examining the relationships between $Z(CH_3)$ and $\Delta E^{\ddagger}$ (Figure 3), therefore, the $Z(CH_3)$ value for ethylene (X = H) should have been divided by 2. Likewise, the $Z(CH_3)$ for benzene would have to be divided by 6 in principle. Practically, however, such cautions have not led to any improvement of the log $Z(CH_3) - \Delta E^{\ddagger}$ relationship. Discarding the symmetry factor in relating the experimental $Z(CH_3)$ to the theoretical $\Delta E^{\ddagger}$ will be permissible in view of the approximate nature of the calculation method used as well as the simplifications of the procedure adopted for the determinations of $Z(CH_3)$.

Acknowledgment. This work was supported in part by the Grants-in-Aid 60303001 and 61303003 from the Ministry of Education, Japan. The authors thank Professor S. Nozakura, Osaka University, for encouragements. They are also grateful to the Computer Center, Instutute for Molecular Science, Okazaki, for an allocation of the CPU time.

Registry No. $H_2C{=}CHOCH_3$, 107-25-5; $H[2C{=}CHCH_3$, 115-07-1; $H_2C{=}CH_2$, 74-85-1; $H_2C{=}CHCO_2H$, 79-10-7; $H_2C{=}C$-HCN, 107-13-1; $H_2C{=}CHC{\equiv}CH$, 689-97-4; $CH_3^{\bullet}$, 2229-07-4.

References and Notes

(1) For example: (a) Yonezawa, T.; Hayashi, K.; Nagata, C.; Okamura, S.; Fukui, K. *J. Polym. Sci.* **1954**, *14*, 312. (b) Hayashi, K.; Yonezawa, T.; Nagata, C.; Okamura, S.; Fukui, K. *J. Polym. Sci.* **1956**, *20*, 537. (c) Fueno, T.; Tsuruta, T.; Furukawa, J. *J. Polym. Sci.* **1959**, *40*, 487. (d) Kawabata, N.; Fueno, T.; Tsuruta, T.; Furukawa, J. *Bull. Chem. Soc.* **1963**, *36*, 1168.

(2) Evans, M. G.; Gergely, J.; Seaman, E. C. *J. Polym. Sci.* **1948**, *3*, 866.

(3) Hehre, W. J.; Lathan, W. A.; Newton, M. D.; Ditchfield, R.; Pople, J. A. QCPE Program No. 236, Indiana University, Bloomington, IN.

(4) Binkely, J. S.; Pople, J. A.; Hehre, J. W. *J. Am. Chem. Soc.* **1980**, *102*, 939.

(5) Herzberg, G. *Electronic Spectra and Electronic Structure of Polyatomic Molecules*; van Norstrand: New York, 1966.

(6) Kamachi, M.; Tanaka, K.; Kuwae, Y. *J. Polym. Sci., Polym. Chem. Ed.* **1986**, *24*, 925.

(7) Ranby, B.; Rebek, J. F. *ESR Spectroscopy in Polymer Research*; Springer-Verlag: Berlin, 1977.

(8) Benson, S. *Thermodynamical Kinetics*, 2nd ed.; Wiley: New York, 1976.

(9) Cvetanović, R. J.; Irwin, R. S. *J. Chem. Phys.* **1967**, *46*, 1694.

(10) Dewar, M. J. S.; Olivella, S. *J. Am. Chem. Soc.* **1978**, *100*, 5290.

(11) (a) Szwarc, M. *J. Polym. Sci.* **1955**, *16*, 367. (b) Leavitt, F.; Levy, M.; Szwarc, M.; Stannett, V. *J. Am. Chem. Soc.* **1955**, *77*, 5493. (c) Buckley, R. P.; Szwarc, M. *J. Am. Chem. Soc.* **1956**, *78*, 5696. (d) Herk, L.; Stefani, A.; Szwarc, M. *J. Am. Chem. Soc.* **1961**, *83*, 3008. (e) Szwarc, M.; Birks, J. H. *Theoretical Organic Chemistry*; Kekule Symposium; Butterworth: London, 1958; pp 271-278.

(12) Fueno, T.; Yokota, S. *Chem. Lett.* **1987**, 1641.

(13) Glasstone, S.; Laidler, K. J.; Eyring, H. *The Theory of Rate Processes*; McGraw-Hill: New York, 1941.

(14) Hammond, G. S. *J. Am. Chem. Soc.* **1955**, *77*, 334.

(15) Nagase, S.; Takatsuka, K.; Fueno, T. *J. Am. Chem. Soc.* **1976**, *98*, 3838. Nagase, S.; Fueno, T. *Bull. Chem. Soc. Jpn.* **1976**, *49*, 2929.

Nonterminated Chain Polymerization in a Convectionless Gas

H. Rabeony and H. Reiss*

University of California, Los Angeles, California 90024. Received June 29, 1987

ABSTRACT: We have investigated the steady-state distribution, with respect to degree of polymerization and location within the reaction chamber, of polymeric radicals produced by a gas-phase free radical chain reaction, under the following conditions. Initiating free radicals are produced, uniformly and at a constant rate, throughout a uniform monomer vapor in a reaction chamber in which the gases are free of convection, and the concentration of radicals is so low that recombinative termination is absent. The free radicals propagate into polymeric radicals which diffuse to the walls of the chamber where they are irreversibly adsorbed. The steady-state distribution results. For a cylindrical chamber with plane-parallel ends, we have been able to achieve an exact analytical result for the distribution even when both the propagation constant and diffusion coefficient depend on the degree of polymerization. Previously, an approximation to this distribution had been used to analyze data (obtained by using nucleation for detection) from styrene vapor, polymerized under the above conditions. We estimate the error in that approximation. The exact distribution is now available for future studies. Achievable degrees of polymerization depend on chamber size, and we illustrate the application of the theory with a simple example.

The Reaction System and Ultraslow Chemistry

It is possible to study[1] free radical, gas-phase chain polymerization under conditions where so few chains grow simultaneously that they cannot encounter one another so as to engage in bimolecular, recombinative termination. Indeed, in the case of styrene, where self-initiated *thermal* polymerization in the gas phase has been clearly demonstrated[1,2] (at room temperature), only between 1 and 200 new chains appear to be initiated in a cubic centimeter each second. More recent, not yet published, studies[3] indicate that other vinyl monomers as well as dienes can be made to polymerize just as sparsely, if the gas is "doped" with an *extremely* small charge of peroxide initiator. Furthermore it appears possible to study ionic chains in the same manner.

Finally, there is the possibility that other kinds of initiators, e.g., metal carbonyls, as well as other kinds of polymers, e.g., inorganic polymers produced by a ringopening mechanism, may be studied in this manner.

These various processes, especially the initiation step, might be described as "ultraslow chemistry". In fact, the growth of the polymer, and the method employed for its detection (nucleation), combine to provide "amplification" of unprecedented magnitude. The consequence is a method not only for the study of polymerization but also for examining the mechanistic chemistry of the very slow initiation step.

The scenario for these phenomena is the following. Gaseous monomer, along with a supporting gas (He, Ar), is enclosed in a chamber upon whose walls polymer is adsorbed irreversibly. *Care is taken to ensure that convection is absent.* Polymer chains are somehow initiated at a constant rate, uniformly throughout the chamber. The growing chains also diffuse. As a result, they are eventually lost to the walls (where they are irreversibly adsorbed). A steady state is established as a balance between initiation and loss to the walls. In this state, the polymer distribution depends on polymer size as well as location within the chamber. Obviously, smaller sizes will dominate at locations close to the wall, since near the walls, growing polymers are more likely to be adsorbed before they become large.

For various reasons,[1,2,4] it is important to know this distribution. In ref 4, an attempt was made to derive it for the case in which the chamber was narrow in one dimension and so wide in the other dimensions that the walls (in those dimensions) could be considered to lie at infinity. In other words, the chamber consisted of two parallel planes. Furthermore, both the diffusion coefficient and the rate constant for the propagation of the polymer were assumed (unrealistically) to be independent of polymer size. This model yielded an exact result for the distribution but, unfortunately, only in terms of an exactly determined generating function which had to be expanded in its basic parameter, before the distribution (contained in its coefficients) could be specified. This expansion became unwieldy after the first few terms.

The difficulty was partly remedied by solving the problem by treating polymer size (approximately) as a continuous variable. The approximation did yield an analytical result, but its degree of error could not be readily estimated.

Since the scenario is important to both gas-phase polymerization and ultraslow chemistry, we reexamine the boundary value problem, involving reaction and diffusion, in the present paper. In particular, we study not a system with infinitely removed side walls as in ref 4 but rather a cylindrical chamber with plane-parallel ends. This shape has been involved in recent experimental studies[1,2,4] and will undoubtedly be important in the future. Furthermore, we allow the diffusion coefficient and propagation constant to depend *arbitrarily* on polymer size. We are able to arrive at an exact analytical solution for the distribution. By comparing the approximate with the exact solution we obtain a measure of its error. Finally, we examine the possibility of generating *isolated* polymers, in the gas phase (as in the case of styrene vapor), large enough to be observed directly by light scattering methods.

Formulation and Solution of the Boundary Value Problem, Exact and Approximate

As indicated in the previous section we shall deal with a cylindrical reaction chamber. Figure 1 will be helpful. The chamber is of radius a and height $2L$. We choose r for the radial coordinate and z for the vertical one and position the chamber such that

$$-L \le z \le L \qquad 0 \le r \le a \tag{1}$$

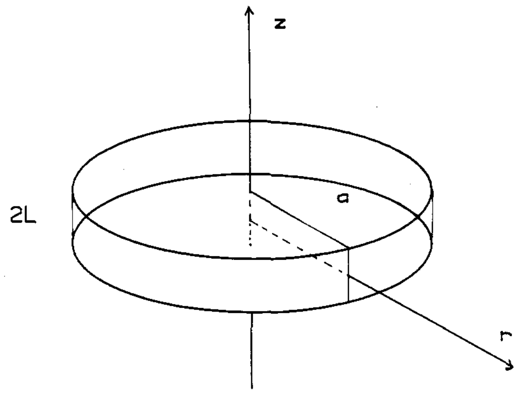

Figure 1. Geometry of the reaction chamber and relevant cylindrical coordinates.

The reactions which take place in the chamber are of the type

$$\begin{aligned} \text{monomer} &\rightarrow \mathrm{R}^\bullet, & &I \\ \mathrm{R}^\bullet + \mathrm{M} &\rightarrow \mathrm{RM}^\bullet, & &k_1[\mathrm{M}]P_1 \\ \mathrm{RM}^\bullet + \mathrm{M} &\rightarrow \mathrm{RMM}^\bullet, & &k_2[\mathrm{M}]P_2 \\ &\text{etc.} \end{aligned} \tag{2}$$

in which $\mathrm{R}^\bullet$ denotes a free radical and M a monomer. $\mathrm{R}^\bullet$, $\mathrm{RM}^\bullet$, and $\mathrm{RMM}^\bullet$ are polymers of sizes 1, 2, and 3 whose concentrations are denoted by P_1, P_2, and P_3, respectively. The appropriate rate expressions are shown at the right of eq 2. I is the initiation rate (molecule $\mathrm{cm}^{-3}\,\mathrm{s}^{-1}$), k_1 and k_2 are rate constants (cm^3 molecule^{-1} s^{-1}) for the propagation of the chain, and [M] is the monomer concentration. Note, in particular, that $\mathrm{R}^\bullet$ is defined to be the polymer of size 1. The various products of the reactions, eq 2, also diffuse to the walls of the chamber with diffusion coefficients D_1, D_2, D_3, etc.

We assume that the steady state has been achieved. Reiterating, we denote the local concentration of polymers of size j (degree of polymerization j) by $P_j(z,r)$ and assume that the constant and uniform rate of initiation (rate of production of free radicals) is I, per cubic centimeter per second. We also let k_j and D_j represent the rate constant for propagation and diffusion coefficient, respectively, both possibly dependent on j. Then, in the steady state, the continuity equations are

$$\frac{1}{r}\frac{\partial}{\partial r}\left(r\frac{\partial P_1}{\partial r}\right) + \frac{\partial^2 P_1}{\partial z^2} - \frac{K_1}{D_1}P_1 + \frac{I}{D_1} = 0$$

$$\frac{1}{r}\frac{\partial}{\partial r}\left(r\frac{\partial P_j}{\partial r}\right) + \frac{\partial^2 P_j}{\partial z^2} - \frac{K_j}{D_j}P_j + \frac{K_{j-1}}{D_j}P_{j-1} = 0, \qquad j > 1 \tag{3}$$

where

$$K_j = k_j[\mathrm{M}] \tag{4}$$

and where [M] is the uniform and time independent (because of the small number of growing polymers) monomer concentration. The appropriate boundary conditions, since the walls act as perfect sinks, are

$$P_j(-L,r) = P_j(L,r) = P_j(z,a) = 0 \tag{5}$$

and

$$[\partial P_j/\partial r]_{r=0} = 0 \tag{6}$$

Equation 6 is required by symmetry. In eq 2, the first two terms represent the net diffusive accumulation of polymers while the last two terms correspond to net reactive accumulation.

We have been able to achieve a rather elegant exact solution to the boundary value problem posed by eq 3, 5, and 6. The method of solution is presented in the Appendix. Here we only present the solution, namely,

$$P_j(z,r) = \sum_{\alpha}\sum_{m=0}^{\infty}\left[\frac{(-1)^m 4I}{D_1 L\alpha J_1(\alpha)\omega_m}\right]\left[\frac{\prod_{i=1}^{j-1}(K_i/D_{i+1})}{\prod_{i=1}^{j}\left[\left(\frac{\alpha}{a}\right)^2+\frac{K_i}{D_i}+\omega_m{}^2\right]}\right](\cos\omega_m z)J_0\left(\alpha\frac{r}{a}\right) \tag{7}$$

where J_0 and J_1 are Bessel functions of order zero and one, respectively, and the quantities α are the sequence of roots of

$$J_0(\alpha) = 0 \tag{8}$$

while

$$\omega_m = \frac{(2m+1)\pi}{2L}, \qquad m = 0, 1, 2, ... \tag{9}$$

It is of interest to examine the solution, eq 7, as $a \rightarrow \infty$, i.e., when the chamber consists of only two plane parallel sheets of infinite extent. Under these conditions the quantity α/a in the denominators of the terms of eq 7 vanishes. Furthermore, the sum

$$\sum_{\alpha}\frac{1}{\alpha J_1(\alpha)}J_0\left(\alpha\frac{r}{a}\right) = \frac{1}{2} \tag{10}$$

appears in the series. This sum can be shown to equal $^1/_2$ by using the orthonormality properties of the Bessel functions (see Appendix). Substituting this value in eq 7 gives

$$P_j(z) = \sum_{m=0}^{\infty}\left[\frac{(-1)^m 2I}{D_1 L\omega_m}\right]\left[\frac{\prod_{i=1}^{j-1}(K_i/D_{i+1})}{\prod_{i=1}^{j}\left[\frac{K_i}{D_i}+\omega_m{}^2\right]}\right]\cos\omega_m z \tag{11}$$

The expressions become especially simple when K_i and D_i do not vary with polymer size. In that case eq 11 becomes

$$P_j(z) = \sum_{m=0}^{\infty}\left[\frac{(-1)^m 2I}{KL\omega_m}\right]\left[\frac{K/D}{\left(\frac{K}{D}+\omega_m{}^2\right)}\right]^j\cos\omega_m z \tag{12}$$

where K and D are the common values of rate constant and diffusion coefficient. The convergence of the series is rapid.

In ref 1 and 4 only the limit $a \rightarrow \infty$ was considered, and in order to have an analytical expression for the distribution, an approximation was introduced, such that the parameter j in eq 3 was assumed to be continuous. This approximation is no longer necessary, since an *exact* analytical expression (in which j remains discrete) is available in eq 7. However, in order to estimate the error in the "continuum" approximation (already used for the analysis of experimental data in ref 1) it is desirable to compare it with the exact result.

For the sake of generality, we first derive the approximate formula for the case in which a is finite, only the case $a \rightarrow \infty$ having been treated in ref 4.

In the approximate treatment of ref 4, K_j and D_j were assumed independent of j. Also, the approximation

$$P_j - P_{j-1} \approx \partial P/\partial j \tag{13}$$

was employed. In eq 13 P is the function $P(z,r,j)$. Finally, $P(z,r,0)$ was *defined* as

$$P(z,r,0) = I/K \tag{14}$$

With eq 13 and 14 and with K_j and D_j equal to the common quantities K and D, respectively, the set of equations in eq 3 may be represented by

$$\frac{D}{K}\left[\frac{1}{r}\frac{\partial}{\partial r}\left(r\frac{\partial P}{\partial r}\right)+\frac{\partial^2 P}{\partial z^2}\right] = \frac{\partial P}{\partial j} \tag{15}$$

with eq 14 as an "initial condition". The boundary conditions are still given by eq 5 and 6 which, in the current notation, may be rewritten as

$$P(-L,r,j) = P(L,r,j) = P(z,a,j) = 0 \tag{16}$$

$$[\partial P/\partial r]_{r=0} = 0 \tag{17}$$

The solution of eq 15, subject to eq 14, 16, and 17, may be obtained straightforwardly by the separation of variables and use of the orthogonality properties of both Bessel functions and Fourier series. The result is

$$P(z,r,j) = \sum_{\alpha}\sum_{m=0}^{\infty}\left[\frac{(-1)^m 4I}{KL\alpha J_1(\alpha)\omega_m}e^{-(D/K)[(\alpha/a)^2+\omega_m{}^2]j}\right]J_0\left(\alpha\frac{r}{a}\right)\cos\omega_m z \tag{18}$$

where α and ω_m have the meanings specified by eq 8 and 9. Once again, the relation contained in eq 10 may be used in passing to the limit $a \rightarrow \infty$, and we find in that limit

$$P(z,j) = \sum_{m=0}^{\infty}\left[\frac{(-1)^m 2I}{KL\omega_m}e^{-D\omega_m{}^2 j/K}\right]\cos\omega_m z \tag{19}$$

This is the same expression as was obtained in ref 4, except that there z ran from 0 to h rather than from $-L$ to L.

To form some estimate of the error in the continuum approximation, we compare eq 19 with eq 12. We see that the two equations are identical, except that in eq 19

$$e^{-D\omega_m{}^2 j/K} \tag{20}$$

appears in place of

$$\left(\frac{K/D}{\frac{K}{D}+\omega_m{}^2}\right)^j = \frac{1}{\left(1+\frac{D\omega_m{}^2}{K}\right)^j} \tag{21}$$

in eq 12.

In the case that

$$D\omega_m{}^2/K \ll 1 \tag{22}$$

it may be seen, from the right-hand side of eq 21, that, indeed,

$$\left(\frac{K/D}{\frac{K}{D}+\omega_m{}^2}\right)^j \approx e^{-D\omega_m{}^2 j/K} \tag{23}$$

so that when eq 22 holds, the approximation is viable. If D/K is of the order of unity, as it is for styrene vapor in the neighborhood of room temperature,[1] then eq 22 is approximately satisfied for $m = 0$ and $L = 2.5$ cm (the value of L appearing in ref 1). For these conditions

$$\frac{D\omega_0^2}{K} = \frac{D}{K}\left[\frac{\pi}{2L}\right]^2 = 0.39 < 1 \tag{24}$$

For vinyl acetate D/K is less than unity and $D\omega_0^2/K$ would even be smaller and the approximation better.

On the other hand, for eq 24 to be useful, the series in eq 12 and 19 should converge so rapidly that only the term corresponding to $m = 0$ need be retained. Because ω_m increases so rapidly with m (e.g., $\omega_1^2/\omega_0^2 = 9$), this is usually the case. It is even more the case as j increases, since the first square-bracketed term in eq 12 and the exponential in eq 19 are raised to the power j.

In any event there is no further need to employ the approximate result.

Illustration of the Application of the Theory

The monomer system, arranged as described in the preceding sections, produces a polymer distribution, steady in both size and space. Indeed, we already know[1] that such a steady distribution is established in styrene vapor, in the neighborhood of room temperature, and significant experiments[1,2] have already been performed on the styrene system. These experiments have been concentrated on the study of the smaller polymers in the distribution, an approach made possible by the enormous amplifying power of the gas-phase nucleation process. These studies should, of course, be continued, but it is important to recognize that, under the proper conditions, there might be substantial numbers of larger polymers in the distribution.

It should be kept in mind that the system is one in which the individual polymer radicals cannot encounter one another. Consequently, they are unable to engage in bimolecular, recombinative termination; they can only be lost to the walls. Also, because they cannot encounter one another, they do not coagulate. Such a system of large, *isolated* gas-phase polymer molecules (indeed, of isolated polymeric *free radicals*), if the polymers can be observed, offers the opportunity to answer a variety of basic scientific questions.

Clearly, the size of the reaction chamber is important. Larger chambers will lead to larger polymers since the walls will be further removed from the bulk of the reacting mixture. On the other hand, with the walls further removed, the local, *total* concentration of radicals (of all sizes) will also be increased, and if this concentration becomes high enough, e.g., on the order of 10^7–10^8 cm^{-3}, recombinative termination will reappear, and the conditions of isolation will be breached. Thus, in increasing the size of the chamber, we work at cross purposes, and there will be an optimum intermediate range of sizes which we need to determine.

Increasing the size of the chamber also makes it more difficult to avoid convection which, in a chamber of reasonable size, can be eliminated by maintaining a small positive vertical temperature gradient. The occurrence of convection would invalidate the formula for the distribution exhibited in eq 7.

For large enough polymers gravitational forces should be taken into account, since these can lead to "settling". (Actually the effects of gravity can be factored into the boundary value problem, and an exact analytical result can still be obtained in place of eq 7, but we do not deal with this complication here.)

In illustrating our theoretical results, it is convenient, in the interest of clarity of visualization, to focus on the case $a \to \infty$, i.e., on a chamber whose walls are two infinite parallel planes, separated by the distance $2L$. There is no special difficulty in treating the case of finite a. However, insofar as both trends and order of magnitude are concerned, no advantages will be introduced by dealing with this more realistic case, and, also, we would lose the simplicity of the more idealized one.

By restricting consideration to $a \to \infty$, we can work with $P_j(z)$ as prescribed by eq 12. As a measure of the total radical concentration we will refer to

$$G(0) = \sum_{j=1}^{\infty} P_j(0) \tag{25}$$

i.e., to the total concentration on the midplane between the walls. An exact expression for G appears as eq 23 of ref 1. There, however, h appears in place of $2L$. In any event, the correct formula is

$$G(0) = 4L^2I/8D \tag{26}$$

Notice that in using eq 12 and 26, we are further idealizing the system so that K_j and D_j are considered to be independent of polymer size.

Since styrene vapor is *already known* to constitute a system of the sort under consideration, we will, for the sake of definiteness, base our calculations on this vapor.

In ref 1 it was found that appropriate values for K and D, in the neighborhood of room temperature, were

$$K = 0.1\ \text{s}^{-1} \qquad D = 0.1\ \text{cm}^2\ \text{s}^{-1} \tag{27}$$

while in the case of I, only upper and lower bounds were provided. These were estimated to be

$$\begin{gathered} I(\text{upper bound}) = 200.0\ \text{molecules cm}^{-3}\ \text{s}^{-1} \\ I(\text{lower bound}) = 1.0\ \text{molecule cm}^{-3}\ \text{s}^{-1} \end{gathered} \tag{28}$$

In the absence of evidence to the contrary, the upper bound was chosen to represent I. This choice was not critical because it was shown in ref 1 (see Table III of that reference) that the determination of K, by the method used in ref 1, was insensitive to the value chosen for I.

Preliminary, unpublished work by Schmitt, mentioned as ref 2, now gives strong indication that I is actually closer to the *lower* rather than the *upper* bound. Thus, for the purpose of the present discussion, we will choose $I = 1.0$ molecule cm^{-3} s^{-1}. This value, together with the values of K and D in eq 27, constitutes the full set of parameter values we shall need.

Before proceeding to investigate the effects of chamber size, we note that eq 12 predicts that with increase of L, $P_j(0)$ "saturates" at a value independent of j. Thus, recalling that ω_m depends inversely on L and letting $L \to \infty$ in eq 12 give the result

$$\lim_{L\to\infty} P_j(0) = I/K \tag{29}$$

As will emerge below, this "saturation" occurs, for all practical purposes, when L is still quite finite; i.e., there is a large but finite value of L for which the walls are effectively infinitely distant from the midplane.

Equation 12 assumes that the steady state has been achieved. In order to estimate the relaxation time to the steady state, we consider an infinite system in which, at a point reasonably distant from the walls, there will be no diffusion. Then, by means of kinetic reasoning alone, it is easy to show that the time dependence of P_j is

$$P_j(t) = \frac{I}{K}[1 - e^{-Kt}\,\exp_{j-1}(Kt)] \tag{30}$$

where t is time and

$$\exp_i(x) = \sum_{n=0}^{i} \frac{x^n}{n!} \tag{31}$$

By use of eq 30, it can be shown that the time for the

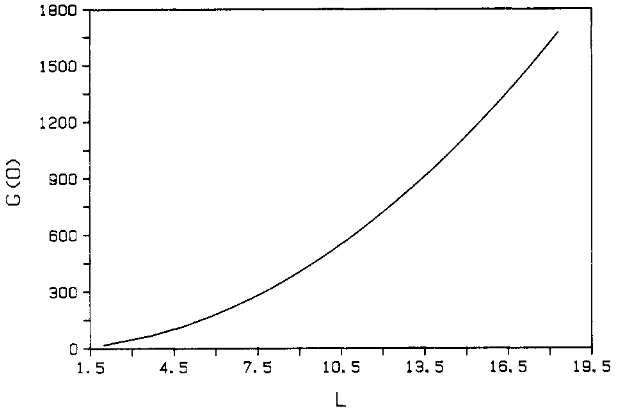

Figure 2. Dependence of total radical concentration (on midplane) on L in centimeters. $K = 0.1\ \mathrm{s^{-1}}$, $D = 0.1\ \mathrm{cm^2\ s^{-1}}$, $I = 1.0$ molecule $\mathrm{cm^{-3}\ s^{-1}}$, and $a = \infty$.

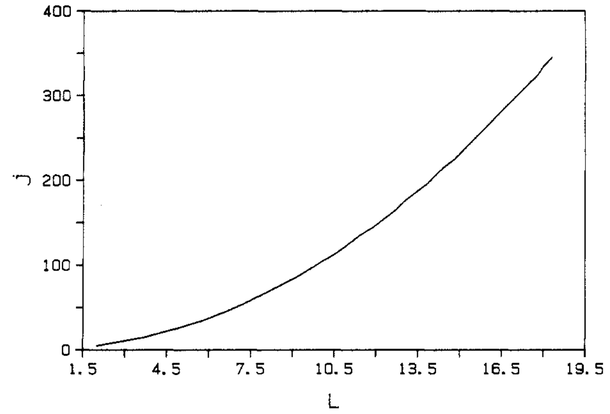

Figure 3. Dependence of the polymer size, j, for which $P_j(0) = 1.0\ \mathrm{cm^{-3}}$, on L in centimeters. $K = 0.1\ \mathrm{s^{-1}}$, $D = 0.1\ \mathrm{cm^2\ s^{-1}}$, $I = 1.0$ molecule $\mathrm{cm^{-3}\ s^{-1}}$, and $a = \infty$.

second term in the curly brackets to vanish, i.e., the relaxation time to the steady state, is on the order of

$$\tau_j = j/K \tag{32}$$

Now we turn to the applications of eq 12 and 26. From, in these equations, the values of K and D in eq 27 and the lower bound for I in eq 28, Figures 2–4 have been generated.

Figure 2 exhibits the dependence of $G(0)$ on L and shows that, even when L is of the order of 17.5 cm, $G(0)$ only attains a value of about 1600 $\mathrm{cm^{-3}}$, far below $10^7\ \mathrm{cm^{-3}}$ where the danger of recombination appears. This means that recombinative termination is not a factor up to chamber sizes which may be so large that eq 12 will allow finite concentrations of large polymers.

To investigate this question, eq 12 was used to calculate the curve exhibited in Figure 3. This is a plot, versus L the chamber size, of the size j of the polymer that, in the steady state, achieves a concentration on the midplane (i.e., $z = 0$) of 1.0 $\mathrm{cm^{-3}}$. Smaller polymers will be present in higher concentrations and larger ones in lower concentrations.

As expected, the size at which a concentration of 1.0 $\mathrm{cm^{-3}}$ is achieved increases with L. In fact, the rate of increase is greater than linear, because concentrations of *all* sizes tend to the *same* value I/K, as required by eq 29 when "saturation" is induced by increasing L. However, from Figure 3 it may be noted that the size, having $P_j = 1.0\ \mathrm{cm^{-3}}$, is already on the order of 400 when the chamber achieves the modest dimension, $L = 19.5$ cm. Equation 32 indicates that the time to achieve the steady state, for a polymer of size 400, is on the order of 4000 s. Clearly, the size at which $P_j = 1.0\ \mathrm{cm^{-3}}$ can be increased dramatically by increasing L beyond 19.5 cm. Finally, reference to Figure 2 shows that, over the entire range of L involved in Figure 3, $G(0)$ is less than 1800 $\mathrm{cm^{-3}}$. Thus we can be assured that recombinative termination will not be a factor.

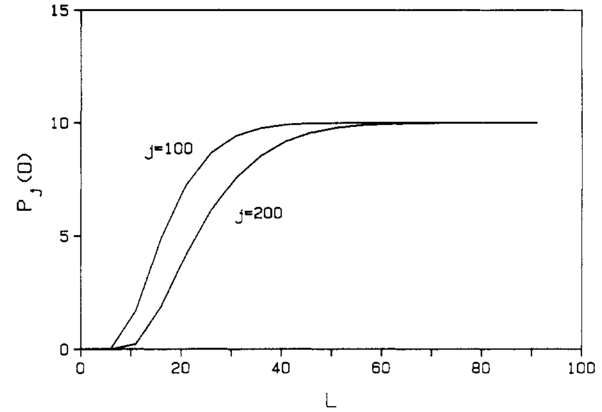

Figure 4. $P_{100}(0)$ and $P_{200}(0)$ versus L in centimeters, showing the "saturation" phenomenon. $K = 0.1\ \mathrm{s^{-1}}$, $D = 0.1\ \mathrm{cm^2\ s^{-1}}$, $I = 1.0$ molecule $\mathrm{cm^{-3}\ s^{-1}}$, and $a = \infty$.

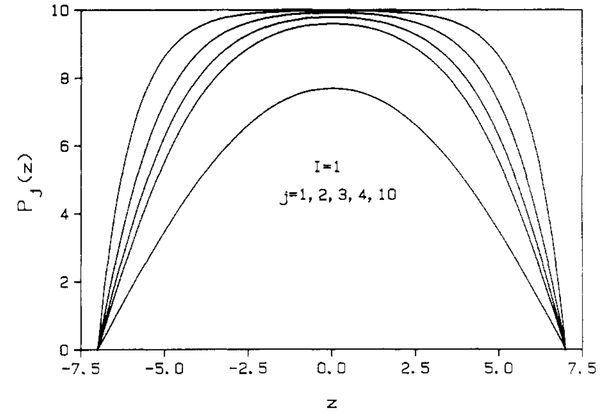

Figure 5. Profiles $P_j(z)$ for $j = 1, 2, 3, 4$, and 10, for $L = 7$ cm and $a = \infty$. $K = 0.1\ \mathrm{s^{-1}}$, $D = 0.1\ \mathrm{cm^2\ s^{-1}}$, and $I = 1.0$ molecule $\mathrm{cm^{-3}\ s^{-1}}$.

Figure 4 shows plots of $P_j(0)$ versus L for $j = 100, 200$. Both plots exhibit the saturation phenomenon, as L is increased. Note that *both* saturate at $P_j(0) = 10\ \mathrm{cm^{-3}}$, i.e., at the common value I/K required by eq 29. Saturation occurs at a smaller value of L, for the curve having smaller j, and *both* curves achieve their plateaus at values of L such that $G(0)$ lies far below the $10^7\ \mathrm{cm^{-3}}$ level at which recombination becomes possible.

Figure 5 details the profiles of P_j across the chamber width, $2L$, for several values of j, i.e., $j = 1, 2, 3, 4, 10$. In this figure, $L = 7$ cm. The plots of $P_j(z)$ show that when j is small, e.g., $j = 1, 2$, or 3, the profiles are "flat" near the midplane. However as j becomes larger, e.g., $j = 10$, the profiles adopt a decidedly cosinusoidal shape. This is a reflection of the more rapid convergence of the series in eq 12 as j increases. When terms beyond the first can be ignored, the profile will be cosinusoidal, since the first term contains the factor $\cos \omega_0 z$.

Acknowledgment. This work was supported by NSF Grant DMR-84-21383.

Appendix

In order to solve the boundary value problem posed by eq 3, 5, and 6, we express $P_j(z,r)$ in the form

$$P_j(z,r) = \sum_{\alpha} \sum_{m=0}^{\infty} [b_m^{(j)}(\alpha) \cos \omega_m z] J_0\left(\alpha \frac{r}{a}\right) \tag{A1}$$

where, as indicated in the body of the text,

$$\omega_m = \frac{(2m+1)\pi}{2L}, \qquad m = 0, 1, 2, ... \tag{A2}$$

and the α are the sequence of roots of

$$J_0(\alpha) = 0 \tag{A3}$$

where $J_0(x)$ is the Bessel function of order zero, a function of its argument x, on the interval

$$0 \le x \le \infty \tag{A4}$$

The quantities $b_m^{(j)}(\alpha)$ are constants, dependent on the parameters m and α.

The boundary conditions, eq 5 and 6, are automatically satisfied by eq A1, since $\cos \omega_m z$ vanishes at $z = \pm L$, while $J_0(\alpha(r/a))$ vanishes at $r = a$, in view of eq A3. Furthermore, eq 6 is satisfied because the derivative of J_0 with respect to its argument vanishes when that argument is zero.

We know that $P_j(z,r)$ can be expressed as the double sum, exhibited in eq A1, because $\cos \omega_m z$ forms a complete orthogonal set on the interval $-2L \le z \le 2L$, while $J_0(\alpha(r/a))$ forms a complete orthogonal set on the interval $0 \le r \le a$. However, unlike many problems involving hermitian operators, the *individual* terms in the double sum are not *themselves* solutions of the boundary value problem, i.e., the individual terms are *not* eigenfunctions of the operators representing the differential equation. On the other hand, the full solution can be expressed by the full series appearing in eq A1.

If the sum over m in eq A1 is denoted by

$$c_\alpha^{(j)}(z) = \sum_{m=0}^{\infty} b_m^{(j)}(\alpha) \cos \omega_m z \tag{A5}$$

then it is well-known[5] that

$$c_\alpha^{(j)}(z) = \frac{2}{a^2[J_1(\alpha)]^2} \int_0^a r J_0\left(\alpha \frac{r}{a}\right) P_j(z,r)\,\mathrm{d}r \tag{A6}$$

where J_1 is the Bessel function of first order. Furthermore, given eq A5, it is well-known that[6]

$$b_m^{(j)}(\alpha) = \frac{1}{L} \int_{-L}^{L} c_\alpha^{(j)}(z) \cos \omega_m z\,\mathrm{d}z \tag{A7}$$

The conditions of orthonormality for the Bessel function are[5]

$$\int_0^a r J_0\left(\alpha \frac{r}{a}\right) J_0\left(\beta \frac{r}{a}\right) \mathrm{d}r = \delta_{\alpha\beta} \frac{a^2}{2} [J_1(\alpha)]^2 \tag{A8}$$

where $\delta_{\alpha\beta}$ is the Kronecke delta. Also it may be shown that

$$\int_0^a r J_0\left(\alpha \frac{r}{a}\right) \mathrm{d}r = \frac{a^2}{\alpha} J_1(\alpha) \tag{A9}$$

From Bessel's equation[5] it follows that

$$\frac{1}{r} \frac{\mathrm{d}}{\mathrm{d}r}\left[r \frac{\mathrm{d}J_0\left(\alpha \frac{r}{a}\right)}{\mathrm{d}r} \right] = -\left(\frac{\alpha}{a}\right)^2 J_0\left(\alpha \frac{r}{a}\right) \tag{A10}$$

Another useful relation, used in the body of the text, is

$$\sum_\alpha \frac{1}{\alpha J_1(\alpha)} J_0\left(\alpha \frac{r}{a}\right) = \frac{1}{2} \tag{A11}$$

This is easily proved by substituting eq A5 into eq A1, replacing $P_j(z,r)$ in that equation by unity, and making use of eq A6 with $P_j(z,r)$ again replaced by unity.

Having listed these relations, we now turn to the solution of the boundary value problem. Begin with the equation for $P_1(z,r)$ in eq 3. Substitute eq A5 into eq A1 and set $j = 1$. Then substitute the result into the equation for $P_1(z,r)$ in eq 3. The result is

$$\sum_\alpha c_\alpha^{(1)} \left[\frac{1}{r} \frac{\mathrm{d}}{\mathrm{d}r} \left[r \frac{\mathrm{d}J_0\left(\alpha \frac{r}{a}\right)}{\mathrm{d}r} \right] \right] + \sum_\alpha \frac{\mathrm{d}^2 c_\alpha^{(1)}}{\mathrm{d}z^2} J_0\left(\alpha \frac{r}{a}\right) - \frac{K_1}{D_1} \sum_\alpha c_\alpha^{(1)} J_0\left(\alpha \frac{r}{a}\right) + \frac{I}{D_1} = 0 \tag{A12}$$

By substitution of eq A10, this becomes

$$\sum_\alpha \left[-\left(\frac{\alpha}{a}\right)^2 c_\alpha^{(1)} + \frac{\mathrm{d}^2 c_\alpha^{(1)}}{\mathrm{d}z^2} - \frac{K_1}{D_1} c_\alpha^{(1)} \right] J_0\left(\alpha \frac{r}{a}\right) = -\frac{I}{D_1} \tag{A13}$$

The quantity in square brackets in eq A13 does not depend on r, and multiplying both sides of eq A13 by $rJ_0(\beta(r/a))$ and integrating between $r = 0$ and $r = a$ give, using eq A8 and A9,

$$\frac{\mathrm{d}^2 c_\beta^{(1)}}{\mathrm{d}z^2} - \left[\frac{\beta^2}{a^2} + \frac{K_1}{D_1} \right] c_\beta^{(1)} = -\frac{2I}{D_1 \beta J_1(\beta)} \tag{A14}$$

This equation may easily be solved directly for $c_\beta^{(1)}(z)$, but we prefer to substitute eq A5, replacing β by α. The result is

$$\sum_{m=0}^{\infty} \left[\left(\frac{\alpha}{a}\right)^2 + \frac{K_1}{D_1} + \omega_m^2 \right] b_m^{(1)}(\alpha) \cos \omega_m z = \frac{2I}{D_1 \alpha J_1(\alpha)} \tag{A15}$$

Substituting

$$g_m^{(1)}(\alpha) = \left[\left(\frac{\alpha}{a}\right)^2 + \frac{K_1}{D_1} + \omega_m^2 \right] b_m^{(1)}(\alpha) \tag{A16}$$

into eq 2 we get

$$\sum_{m=0}^{\infty} g_m^{(1)}(\alpha) \cos \omega_m z = \frac{2I}{D_1 \alpha J_1(\alpha)} \tag{A17}$$

We can now use eq A7 with $g_m^{(1)}(\alpha)$ replacing $b_m^{(1)}(\alpha)$ and $2I/D_1\alpha J_1(\alpha)$ replacing $c_\alpha^{(1)}(z)$ to evaluate $g_m^{(1)}(\alpha)$. Then, substituting the result into eq A16 gives

$$b_m^{(1)}(\alpha) = \frac{(-1)^m 4I}{D_1 L J_1(\alpha) \omega_m \left[\left(\frac{\alpha}{a}\right)^2 + \frac{K_1}{D_1} + \omega_m^2 \right]} \tag{A18}$$

Finally, this result may be substituted into eq A1 to yield the formula for $P_1(z,r)$ contained in eq 7 in the body of the text.

We now move to the equation for $P_2(z,r)$ in eq 3. Substitute $P_2(z,r)$ expressed in the form eq A1 into that equation, using that form for $P_1(z,r)$ in the last term on its right. Also substitute eq A5 and A10, multiply through by $rJ_0(\beta(r/a))$ as before, and integrate over r between 0 and a. After the orthonormality condition, eq A8, has been applied, we obtain

$$\frac{\mathrm{d}^2 c_\alpha^{(2)}}{\mathrm{d}z^2} - \left[\left(\frac{\alpha}{a}\right)^2 + \frac{K_2}{D_2} \right] c_\alpha^{(2)} = -\frac{K_1}{D_2} c_\alpha^{(1)} \tag{A19}$$

Then, resubstituting eq A5 on both sides of eq A19, performing the differentiation with respect to z, and collecting terms, we arrive at the result

$$\sum_{m=0}^{\infty}\left\{\left[\left(\frac{\alpha}{a}\right)^2+\frac{K_2}{D_2}+\omega_m^2\right]b_m^{(2)}(\alpha)-\frac{K_1}{D_2}b_m^{(1)}(\alpha)\right\}\cos \omega_m z = 0 \qquad \text{(A20)}$$

Since the cos $\omega_m z$ is an orthogonal function, eq A20 can only be satisfied when the coefficient in brackets is identically zero. This leads to the relation

$$b_m^{(2)}(\alpha) = \frac{\dfrac{K_1}{D_2}b_m^{(1)}(\alpha)}{\left[\left(\dfrac{\alpha}{a}\right)^2+\dfrac{K_2}{D_2}+\omega_m^2\right]} = \frac{\dfrac{K_1}{D_2}\left[\dfrac{(-1)^m 4I}{D_1 L\alpha J_1(\alpha)}\right]}{\omega_m\left[\left(\dfrac{\alpha}{a}\right)^2+\dfrac{K_1}{D_1}+\omega_m^2\right]\left[\left(\dfrac{\alpha}{a}\right)^2+\dfrac{K_2}{D_2}+\omega_m^2\right]} \qquad \text{(A21)}$$

where we have used eq A18.

The equation for $P_3(z,r)$ in eq 3 is of exactly the same form as that for $P_2(z,r)$, except that P_3 replaces P_2 while P_2 replaces P_1. The steps leading to the first equation in eq A21 can therefore be repeated with the result

$$b_m^{(3)}(\alpha) = \frac{\dfrac{K_2}{D_3}b_m^{(2)}(\alpha)}{\left[\left(\dfrac{\alpha}{a}\right)^2+\dfrac{K_3}{D_3}+\omega_m^2\right]} \qquad \text{(A22)}$$

and eq A21 may be substituted into this result. Continuing in this manner out to the equation for $P_j(z,r)$, we arrive at

$$b_m^{(j)}(\alpha) = \left[\frac{(-1)^m 4I}{D_1 L\alpha J_1(\alpha)}\right]\left[\frac{\prod_{i=1}^{j-1}(K_i/D_{i+1})}{\omega_m \prod_{i=1}^{j}\left[\left(\dfrac{\alpha}{a}\right)^2+\dfrac{K_j}{D_i}+\omega_m^2\right]}\right] \qquad \text{(A23)}$$

Substitution of this result back into eq A1 gives $P_j(z,r)$ in eq 7 in the body of the text. Thus the problem of the distribution is solved. It is evident that the series in eq 7 is rapidly convergent, because both α and ω_m increase rapidly, in sequence, and the squares of these quantities appear in the denominators of the terms in the series. Furthermore, as j increases the convergence is even more rapid since j square bracket factors appear in the denominators.

Registry No. $C_6H_5CH{=}CH_2$, 100-42-5.

References and Notes

(1) El Shall, M. S.; Bahta, A.; Rabeony, H.; Reiss, H. *J. Chem. Phys.* **1987**, *87*, 1329.

(2) Private communication to the authors from Professor John Schmitt, University of Missouri at Rolla. Professor Schmitt has been conducting measurements on the steady-state distribution of polymeric radicals in styrene vapor, using the high-precision expansion cloud chamber developed at Rolla. Preliminary results (as with the experiments of ref 1) provide definitive evidence of the self-initiated polymerization of styrene in the gas phase. The results also indicate that a time on the order of 10 min is required to set up the steady-state distribution, after the larger polymers are removed by adiabatic expansion and nucleation. Preliminary data, kindly supplied to the authors by Professor Schmitt, when substituted into the formulas of the present paper, suggest that the thermal rate of generation of initiating free radicals is of the order of 1.0 $cm^{-3}\,s^{-1}$.

(3) Unpublished experimental studies, in progress at UCLA, due to M. S. El Shall and the authors.

(4) Reiss, H.; Rabeony, H. M.; El Shall, M. S.; Bahta, A. *J. Chem. Phys.* **1987**, *87*, 1315.

(5) Arfken, G. *Mathematical Methods for Physicists*; Academic: New York, 1968; Chapter 11.

(6) Reference 5, p 511.

Photoresponsive Vinyl Polymer Bearing Norbornadiene as a Pendant Group

Hiroyoshi Kamogawa* and Makoto Yamada

Department of Applied Chemistry, Yamanashi University, Kofu 400, Japan.

Received June 5, 1987

ABSTRACT: The synthesis of a novel class of photoresponsive polymers is reported. The norbornadiene unit in the polymer was found to be converted in the film state under nitrogen atmosphere to a quadricyclane unit reversibly with irradiation by UV light of two different wavelengths. Polymers bearing norbornadiene units having carboxylate and/or substituted amide groups at the 2- and 3-positions and having a vinyl group at the end of the 2-substituent were prepared by the polymerization of respective monomers. Polymers bearing an amide substituent at the 2-position indicated a much higher photosensitivity in the film state as well as a larger red shift in the absorption spectrum than those bearing a carboxylate substituent.

Introduction

In a previous study,[1] we reported the first synthesis together with photosensitivity of a vinyl polymer bearing a norbornadiene unit as a pendant group.

In the present study, the carboxylate and/or carboxamide groups bearing a vinyl double bond have been substituted at the 2,3-positions of norbornadiene, and the photosensitivity of the films made of the polymerization products of the resulting vinyl monomers was investigated.

The synthesized monomers were shown in Chart I. Monomers **1a–j** were polymerized to afford respective polymers which gave transparent films from solutions. The polymers thus prepared were irradiated either in solution or in film with UV light under nitrogen atmosphere and

0024-9297/88/2221-0918$01.50/0